

## $^3\text{He}$ Neutron Spin Filter cell development program at JCNS

This content has been downloaded from IOPscience. Please scroll down to see the full text.

2014 J. Phys.: Conf. Ser. 528 012015

(<http://iopscience.iop.org/1742-6596/528/1/012015>)

View [the table of contents for this issue](#), or go to the [journal homepage](#) for more

Download details:

IP Address: 134.94.122.242

This content was downloaded on 06/05/2015 at 13:08

Please note that [terms and conditions apply](#).

## <sup>3</sup>He Neutron Spin Filter cell development program at JCNS

Z Salhi<sup>1</sup>, E Babcock<sup>1</sup>, P Pistel<sup>2</sup> and A Ioffe<sup>1</sup>

<sup>1</sup> Jülich Centre for Neutron Science, Forschungszentrum Jülich GmbH, Outstation at MLZ, Lichtenbergstrasse 1, 85747 Garching, Germany.

<sup>2</sup> Forschungszentrum Jülich GmbH- Engineering und technologie (ZEA-1) Wilhelm-Johnen-Strasse, 52425 Jülich, Germany.

E-mail: [z.salhi@fz-juelich.de](mailto:z.salhi@fz-juelich.de)

**Abstract:** In order to produce high-quality <sup>3</sup>He Neutron Spin Filters (NSF) with a high polarisation level, it is necessary to achieve a long <sup>3</sup>He relaxation time by the reduction of the wall relaxation. This requires one to minimise the amount of impurities at the surface of the glass cells, and to have as few contaminants as possible in the gas filling system. In this report we describe the detailed procedure we employ to produce <sup>3</sup>He cells using our newly built filling station. The obtained life times for a number of cells are practically approaching the fundamental limit imposed by the dipole-dipole interaction between <sup>3</sup>He atoms.

### 1. Introduction

High-quality <sup>3</sup>He Neutron Spin Filters (NSF) should provide a high polarization and a low absorption of neutron beams; this requires one to achieve high levels of <sup>3</sup>He polarization in the <sup>3</sup>He cells (containers). The achieved level of <sup>3</sup>He polarization is defined, from one hand by the rate of the build-up of <sup>3</sup>He polarization and, and from the other by relaxation processes that result in polarization decay. Indeed, a high performance NSF should combine an optimized optical pumping system and <sup>3</sup>He cells (containers) providing minimal achievable polarization losses.

Therefore, parallel to the developments of optimal optical pumping methods [1-4] aiming to the increase the maximum levels of polarization, the development of <sup>3</sup>He cells (containers) close to ideal, i.e. with minimum the <sup>3</sup>He relaxation possible, is necessary. These cells should be optimised to reach a high starting <sup>3</sup>He polarisation and to have very low relaxation rate ( $\Gamma_1=1/T_1$ ) to maintain the <sup>3</sup>He polarisation in the NSF for long time.

Even for perfect cell containers, the decay of <sup>3</sup>He polarisation will result in the decrease of neutron polarisation and transmission. Therefore, especially for offline-polarised cells, this decay ideally must be kept to the lowest possible minimum during the experiment. This in turn limits the number of times one has to repolarise the <sup>3</sup>He cell or refill it while maximizing neutron performance over any given interval of time. Note that all cells are not identical, therefore determining the exact neutron performance requires each of them to be characterised before or after the usage in the experiment and be monitored over time.

The SEOP method also gives the possibility to polarize the <sup>3</sup>He online and in this way balance the <sup>3</sup>He spin-relaxation with continual polarization [5]. Since both the SEOP [6] and MEOP [7] method have been shown to give comparable maximum polarizations, optimized online polarization would provide the highest average performance over time as long as the laboratory maximum



polarization can be maintained in steady state, or near steady state over time with online polarization. Additionally, when using on-line optical pumping, one can limit how often  $^3\text{He}$  cell calibrations must be performed as the relative polarization can be monitored via NMR for possible drifts, and the cells  $^3\text{He}$  pressure is fixed in the typically permanently sealed SEOP cell. Regardless, the smaller the total relaxation rate in a given  $^3\text{He}$  cell, the greater the level of the achievable steady state  $^3\text{He}$  polarisation will be, and thus provide the best possible neutron performance, thus good cell preparation is paramount.

In practice, the wall relaxation is an important process; it can dominate the  $^3\text{He}$  spin relaxation rate or limit eventual performance if care is not taken. Collisions of  $^3\text{He}$  atoms with ferromagnetic impurities at the cell surface as well as the diffusion of  $^3\text{He}$  into the glass may cause relaxation because of the precession of the helium magnetic moment about the net local gradient field caused by the magnetic impurities. Additionally for the SEOP process, there are temperature-dependent wall relaxation processes limiting the maximum steady state polarization [8]. If this optical pumping related relaxation can be lowered it would further increase the absolute polarization performance of SEOP polarized cells. Exploring this parameter with our cells will be the focus of future work.

In the following discussion, we will describe the fabrication process of cells made from GE180 glass and our new gas filling system built to clean cells and fill them with highly pure  $^3\text{He}$  and  $\text{N}_2$ . Then we provide a summary of the main relaxation characteristics and properties of the cells produced. One highlight of this work is that long wall relaxation time cells are now produced routinely in the lab.

## 2. $^3\text{He}$ relaxation processes in $^3\text{He}$ NSF

The  $^3\text{He}$  polarization in the  $^3\text{He}$  NSF cell decays to thermal equilibrium with the characteristic time constant  $T_1$ . The longitudinal relaxation rate  $\Gamma_1 = T_1^{-1}$  results from three main mechanisms for the relaxation of spins:

$$\Gamma_1 = \frac{1}{T_1} = \frac{1}{T_1^{dipole}} + \frac{1}{T_1^{grad}} + \frac{1}{T_1^{wall}}. \quad (1)$$

Here  $T_1^{dipole} = 1/807$  (hours) is the dipole-dipole relaxation time due to the interaction between colliding  $^3\text{He}$  atoms [9]. The magnetic dipole coupling of atoms during a binary collision results in the loss of nuclear polarisation. This relaxation is the fundamental physical process, which ultimately limits the total  $^3\text{He}$  spin relaxation rate.  $T_1^{grad}$  is the relaxation time due to the non-zero gradient of the holding magnetic field and given by:[10-13]

$$\frac{1}{T_1^{grad}} = \frac{7000}{P} \left( \left( \frac{gradB_x}{B} \right)^2 + \left( \frac{gradB_y}{B} \right)^2 \right). \quad (2)$$

Where  $gradB_x$  and  $gradB_y$  are the orthogonal gradients of the static holding field  $B$ , and  $P$  is the  $^3\text{He}$  pressure in bar. For example, with a magnetic field gradient  $gradB/B \leq 10^{-4} \text{ cm}^{-1}$  the  $T_1^{grad}$  is more than 14286h at 1 bar. This value will be used later on this paper as a negligible value for the measurement of the total relaxation time given by Eq.(1) for the practical purposes of this paper. The last term,  $T_1^{wall}$ , is the relaxation time due to the interactions of  $^3\text{He}$  atoms with the cell walls [14-15].

This relaxation is presumably determined by the quality of the glass and possible impurities on its surface and the  $^3\text{He}$  interactions with them. The glass itself can contain small magnetic impurities like magnetite (the most common impurity in glass), and impurities may be introduced in the cell manufacture and preparation. Then, the diffusion of helium into the glass and to the surface may cause relaxation because of the precession of the helium magnetic moment about the net local gradient field caused by the magnetic impurities [14]. The relaxation properties of  $^3\text{He}$  on glass may be related to the permeability of the glass, for cells made of Pyrex (borosilicate) glass which has high  $^3\text{He}$  permeability,

such relaxation process can be as fast as 1 hour. Allumosilicate glasses are known to have lower  $^3\text{He}$  permeability than quartz or Pyrex, that is perhaps why GE180, a boron free allumosilicate glass and the glass of choice for many neutron applications and our  $^3\text{He}$  cells, gives good performance with respect to  $^3\text{He}$  relaxation rates. Fortuitously, GE180 being boron-free, has a low neutron absorption is thus also suited to neutron spin filter applications. Discussions of  $^3\text{He}$  interactions with glasses and coated surfaces are given in refs [16-18], although unfortunately some references did not study GE180, we assume it to have similar properties to the other allumosilicate but boron containing glasses Corning 1723 and 1720 listed in those works.

### 3. Cell fabrication and filling

We have completed a cell filling station, and cell filling procedure borrowing heavily from the experience and results of NIST [19] and ISIS colleagues [20]. The following sections describe our cell fabrication, preparation, and filling procedure as well as the gas ultra pure gas handling and filling station.

#### 3.1. Cell fabrication and filling.

All our cells are blown from semi-custom large diameter ca. OD=24 mm GE180 glass tubing in the glass workshop of the Forschungszentrum Jülich GmbH. One starts from the glass tubing that is reblown to the desired geometry and annealed at  $\sim 785^\circ\text{C}$  for several hours to remove residual stress in the glass. Then cells undergo safety testing up to a typical pressure of 6 bar.

Each cell is cleaned before being attached to a glass manifold or “string” made from O.D.=12.7 mm Pyrex tubing (Figure1). The cleaning procedure involves several steps: (i) a rinse with soapy water, (ii) several rinses with distilled water and (iii) final rinse with methanol to remove water. The string also contains two ampoules of alkali metals (1g pre-scored ampoules Rb and K-Strem Chemicals 99.9+% purity) [21]. Two small bulbs serve as reserve volumes between the cell and the alkali metal ampoules and glass-encased ferrous slugs for breaking the ampoules while inside the sealed string. The emptied ampoules and slugs are removed or “pulled-off” from the string after intermediate distillation of the alkali-metal into the reserve volume.

The entire string, after attaching the cleaned cell to it and putting in the alkali/metal ampoules and ferrous slugs, is connected to the filling station by inserting the open end of the tube into a UHV Swagelock Ultra-Torr™ connection which serves as the adapter from the glass to the vacuum system of the filling station. Connected to this Ultra-Torr fitting is a short SS bellows which helps insure the glass isn't strained or broken during the baking/filling process, and also allows one to pick up and move the string as needed while working with the cell.

Before filling the cells, the system is leak tested with  $^4\text{He}$  gas and baked for several days to achieve the residual pressure as low as  $10^{-9}$  mbar. The cells are baked at  $400^\circ\text{C}$  and evacuated for at least four days to minimise the impurities on the surface of the glass. The cell string is also baked during this time but at a lower temperature of  $200^\circ\text{C}$ , being careful not to overheat or burn the alkali-metal ampoules. After the pressure in the system reaches equilibrium, the valves between the vacuum system and the gas handling system are closed. The alkali-metal ampoules are then broken under vacuum using a magnet and the ferrous slug which is encased in glass to avoid contamination of the cell with ferromagnetic impurities. The slug is lifted with an external magnet and then dropped onto the tip of the break-seal ampoule with the aide of gravity to open it.

Next, the alkali metal is distilled first to a small bulb (Figure1) in the string using a  $530^\circ\text{C}$  1.6 kW hot air gun. After this first distillation, the emptied alkali metal ampoules and the portion of the string containing the ferrous slug are removed via sealing-off the connection between the ampoule and the reservoir bulb with a torch. Afterward, the alkali metals are distilled again, this time into the cell until an opaque coating is observed, first with the K and then with a smaller amount of Rb in the desired ratio.

Now the cell can be filled with the required amount of  $\text{N}_2$  typically 100 mbar, and  $^3\text{He}$  through the getters and a liquid nitrogen cold trap in the glass string to ensure a high gas purity. During the

filling process the cell pressure is monitored using the high precision MKS Baratron pressure transducer (Figure 2) with the accuracy of about 0.05%. For cells with final pressure over atmosphere, the cells are partially submerged in liquid nitrogen until the pressure is low enough ( $<1$  bar) to seal it with the torch in air; this allows for a maximum total cell pressure of about 3.7 bar. Finally, the filled cells are sealed by a torch and pulled-off from the vacuum manifold. Pictures of some of our typical blown cells are shown in Figure 3.

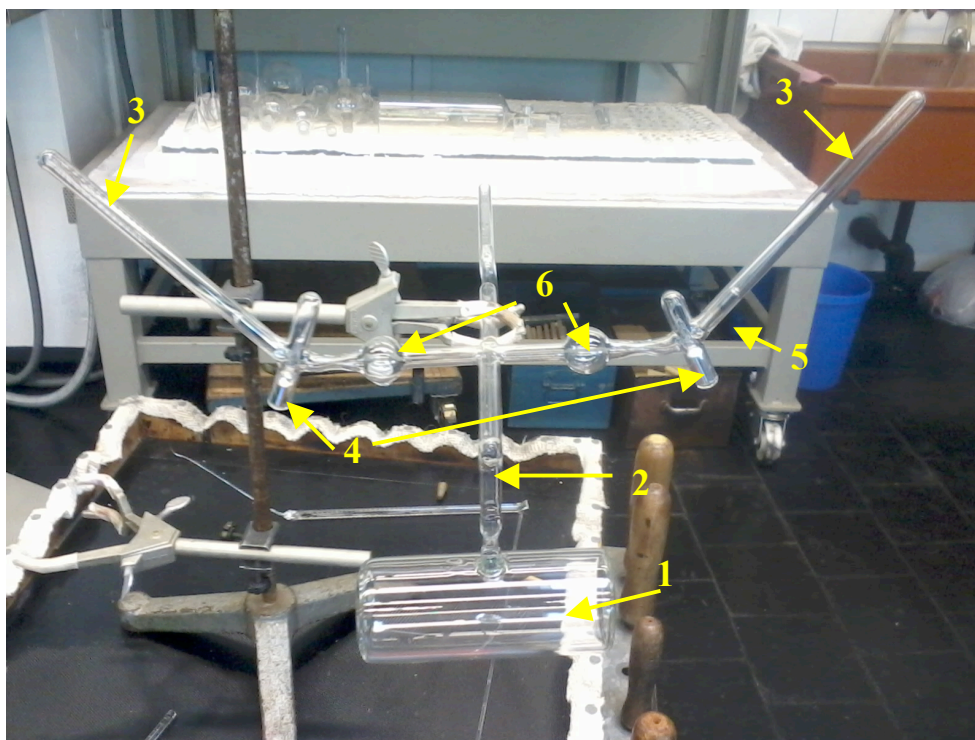


**Figure 1.** The 5 cm x 15 cm cell named Goldorak (1) attached to a Pyrex string (2), the slanted-vertical pull-off (3) containing alkali metal ampoules, Rb left and K right (4), and the ferrous slug (5) sealed within glass. The small bulbs (6) are the reserve volumes, between these bulbs and the ampoules there is a restriction used to pull-off the emptied ampoules and ferrous slugs before the second distillation of the alkali-metal into the cell.

**3.2. Cell filling station.** The cell filling station consists of three main sections: a gas handling system, a high vacuum system, and a gas recovery system as shown in (Figure 2). These three components are described in the following sub-sections.

**A. Gas handling system.**  $^3\text{He}$  and  $\text{N}_2$  gases are provided via 6mm gas tubing, all connections are metal-sealed mostly Swagelock compression fittings. Each gas line has a SAES PS2-CG50 getter and a  $0.5 \mu\text{m}$  particle filter for purifying the gas. The flow-rate is controlled by a pressure reducer placed at the output of each bottle followed by a needle valve.

**B. High vacuum system.** The high vacuum is obtained using two pumps: a Pfeifer “Adixen” pump model P0385E4 (oil-free), which can pump the system from atmospheric pressure down to  $10^{-3}$  mbar and also acts as the backing pump for a Pfeifer Hicube 80 Pro turbo molecular vacuum pump, which allows to achieve pressures as low as several  $10^{-9}$  mbar.

**C. Gas recovery system.** A helium tight piston compressor from KNF Neuberger, model PM24721-286.13, which has been specially sealed and modified by the company for use as a  $^3\text{He}$  compressor [22], is used to collect the gas remaining in the tubes of the gas handling system; the gas is then compressed into a steel gas bottle up to 12 bar. The  $^3\text{He}$  is then separated from impurities using a Zeolite molecular sieve adsorbent at 77 °K followed by a cold head at 8 °K [23]. The gas recovery system is always kept under a high vacuum ( $\sim 10^{-9}$  mbar) to ensure its clearness and that  $^3\text{He}$  gas will not be contaminated by impurities that may later affect the  $^3\text{He}$  optical pumping or cell performance.

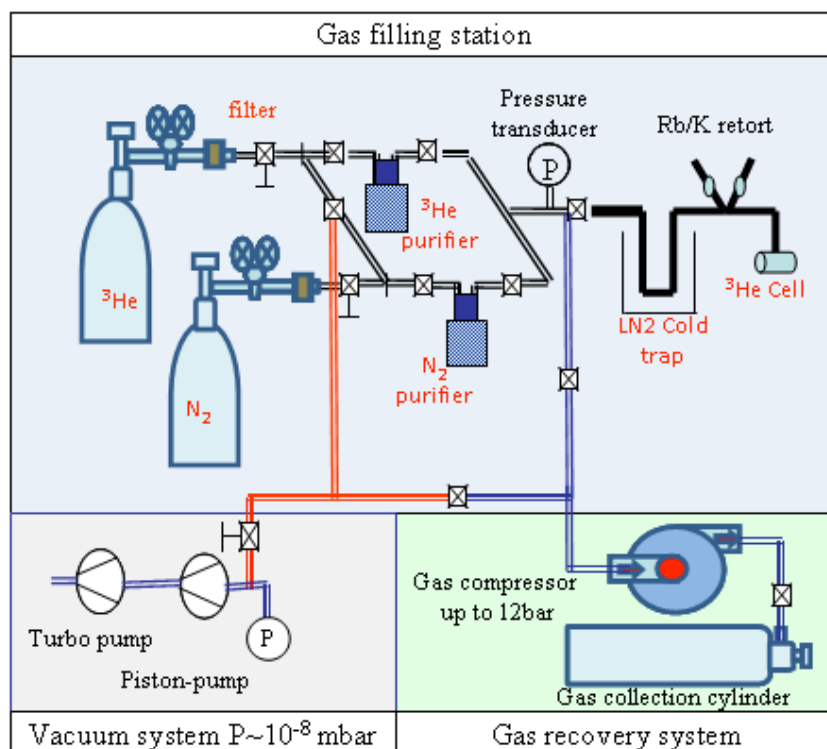


**Figure 2.** Schematic diagram of the cell preparation system, including the oil-free high vacuum system, the filling station and the recovery system.

#### 4. Cell relaxation time measurement procedure and results.

The  $^3\text{He}$  cells are polarized using the SEOP technique [1]. For this purpose a cell is placed in a long 2.2 m 6 coil set of 1.4 m diameter. This can provides a magnetic field of up to 18 G (10 G is normal used) at the centre with a designed field homogeneity  $gradB/B \leq 10^{-4} \text{cm}^{-1}$  in a large volume of about  $(1 \times 0.5 \times 0.5) \text{m}^3$ . The cell are heated, to temperatures up to 220°C, used to achieve a suitable alkali-metal density using a flowing air oven and are illuminated with circularly polarised light from high power,  $P > 90 \text{ W}$ , diode lasers which are spectrally narrowed by chirped volume Bragg gratings (VBG) to achieve a stable linewidth of about 50 GHz at the Rb  $D_1$  optical transition at 794.7 nm (with one particular grating in fixed position, we obtained a linewidth of 35 GHz at 40A or 16.3W output with a linear increase in linewidth of about 1GHz per Ampere to 113 GHz at 120A or 92.5 W output).

The build-up and the decay of the  $^3\text{He}$  polarisation are monitored using NMR free induction decay (FID): the amplitude of the FID signal is proportional to the  $^3\text{He}$  polarisation [11, 24]. The measurements are carried out periodically, typically every hour. The exponential decay fit of the FID

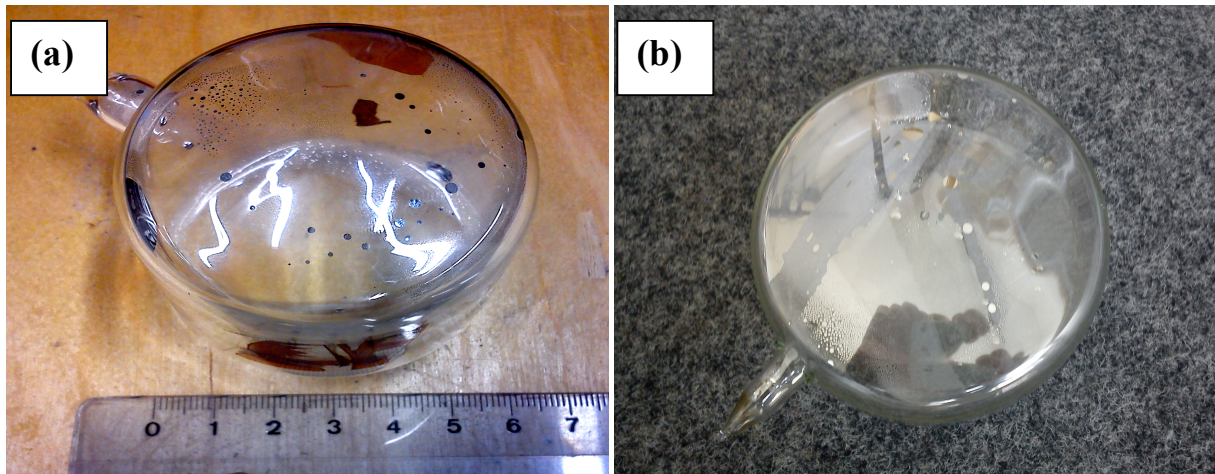


**Figure 3.** Examples of  $^3\text{He}$  NSF cells produced using our new filling station: (a) Puck, diameter 6 cm, length 5 cm and (b) Asterix diameter of 12cm, length 5 cm (see Table 1).

amplitude time-dependence gives the value of  $T_1$ ; for a long  $T_1$  on the order of hundreds of hours, a reliable measurement typically takes several days (see Figure 4.). We generally acquire  $T_1$  decay data for several days until the uncertainty in the exponential fit to the data is under 10%.

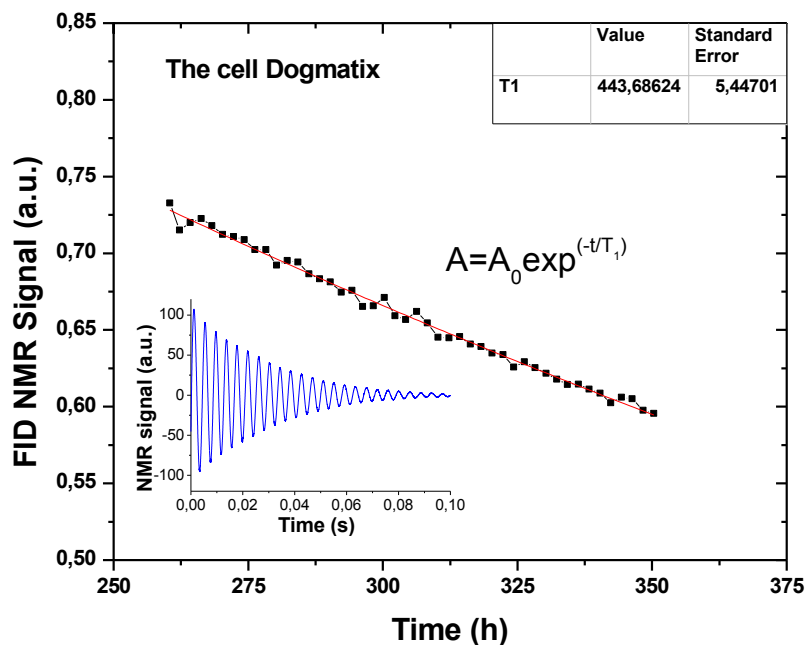


**Figure 4.** Example of the time dependence of the relative polarisation measured with FID NMR and the exponential fit allowing for the determination of the relaxation time  $T_1$

Parameters of a number of  $^3\text{He}$  cells made in our lab using the new filling station are presented in Table 2. As one can see, the measured  $T_1$  is regularly approaching the dipole limit for many of the cells, however we must fully characterize the  $^3\text{He}$  pressures of the sealed cells, this is readily done by measuring the  $1/\nu$  dependent neutron absorption of the cells [25]. Initial test have yielded pressure values 5-10% lower than the fill pressure for Asterix and Willy, further work must be done to characterize the cells pressures in this way and eliminate possible systematic errors. On an interesting side note, even with corrections for the actual  $^3\text{He}$  pressure, some of these cells may exhibit measured  $^3\text{He}$   $T_1$  lifetimes closer to the dipole-dipole limit of than those cited in [26, 27], thus more accurate characterization of them could help to place new experimental limits on the magnitude of axion monopole-dipole coupling strengths as described in those works [26, 27]. However we must also experimentally verify the field gradients in our field coils because from eq. 1, a value at the upper limit of  $1 \times 10^{-4} \text{ cm}^{-1}$  could decrease our measured  $T_1$  lifetimes by on the order of 5% which should be taken into account for such an analysis.

We quickly note, the first two cells in the table, Maja and Puck have been filled in the beginning of the operation of our filling system while it was still under the cleaning process. The cell Homer, because of the big size and the complexity of the cell geometry (toroid or “doughnut” shape), required an unusually long time period for the glass blowing work and more intrusion with the torch on the glass are is required; therefore it is reasonable to assume more impurities could be embedded into the glass during this process. Nevertheless the obtained relaxation time is very satisfactory for practical purposes.

Cell	Size D x L (cm x cm)	Fill pressure (bar)	$T_1$ (hours)	$T_1^{dipole}$ (hours)
Maja	5 cm x 5 cm	0.93	550	860
Puck	6 cm x 5 cm	1	500	800
Kurt	6 cm x 5 cm	2.3	350	350
Willy	6 cm x 5 cm	2.3	350	350
Asterix	12 cm x 5 cm	2.7	280	295
Obelix	12 cm x 5 cm	2.1	330	380
Idefix	12 cm x 8 cm	1.7	380	470
Dogmatix	12 cm x 8 cm	1.8	440	445
Homer	22 cm x 8 cm	0.5	1070*	1600
Thekla	8 cm x 5 cm	2.3	290	350
Goldorack	5 cm x 15 cm	2.7	230	295

**Table 1.** Parameters of different  $^3\text{He}$  glass cells produced at the JCNS. D and L are the inner diameter and length respectively. The fill pressure is the deduced pressure from the Baratron pressure sensor during cell filling. Many cell pressures have not yet been calibrated via. neutron absorption measurements however initial measurements on Willy and Asterix implied pressures 5-10% lower than the fill pressure. More conclusive measurements will be done at a later time. The uncertainty in the  $T_1$  measurements is  $\pm 10$  hours. \*If one assumes a gradient of  $1 \times 10^{-4} \text{ cm}^{-1}$  in our field coils, for Homer, because of the 0.5 bar pressure the  $T_1$  in a theoretical gradient-less field could be up to 200 hours longer.

## 5. Development of wide-angle GE180 cells suitable for SEOP and MEOP

The use of sealed (or fully blown)  $^3\text{He}$  cells made of GE180 glass [13] could vastly simplify the equipment required for wide-angle polarization analysis as this would allow the direct polarization of the cell using the SEOP method. Furthermore, fully blown GE180 glass cells may indeed have

practical advantages such as pressure resistance and durability compared to other proposed routes such as to form cells from bonded or glued together flat and curved plates of crystal silicon, quartz or even GE180 [28, 29]. Presumably cells made of GE180 could be used as sealed cells to be polarized directly with a SEOP polarizer system as in [29] or to be used as so-called valved cells [28, 30] that are filled with pre-polarized  $^3\text{He}$  gas from a large scale  $^3\text{He}$  polarizer employing either the MEOP or SEOP techniques [1-4]. Most likely, silicon or quartz cells are only suitable to be used as valved cells referencing the experience of the NIST, ILL, and ISIS groups which have worked on such cells [29, 30, 28] although we have not pursued these techniques ourselves.

We have successfully manufactured a number of fully blown GE180 wide-angle  $^3\text{He}$  spin-filter cells. These unique cells have been produced in the glass workshop of the Forschungszentrum Jülich. GE180 is again chosen because of its neutron compatibility and because it is the best experimentally known material for providing long  $T_1$  relaxation times of the  $^3\text{He}$  gas and maximum polarization using the SEOP method.

A very first all blown “C” or “banana” shaped GE180 cell is shown in the Figure 5a. In Figure 5b a doughnut-shaped blown GE180 cell with a trapezoidal cross section more suitable for a small sample and large area-detector geometry is shown, the trapezoidal cross section shape is also useful to minimise the  $^3\text{He}$  volume of the cell without affecting the solid angle covered. The C-shaped cells are made by sealing off two points of the doughnut cells. In Figure 6a the picture of a very large (external diameter of 22 cm) doughnut-shaped cell called Homer is shown. This cell was prepared with a Rb and K mixture for hybrid pumping [8] with the procedure described in the previous section. Being intended only for testing of  $^3\text{He}$  relaxation times of a new Magic-PASTIS coil system [31], it contains 0.5 bar of  $^3\text{He}$ : the lower  $^3\text{He}$  pressure makes the cell rather sensitive to the magnetic field gradient relaxation,  $T_1^{grad}$  (Eq. (1)), and is thus a good probe for the optimization of the performance of the Magic-PASTIS magnetic cavity. The cell Homer was measured to have  $T_1=1074$  hours in what we presume to be an “ideal” reference magnetic holding field (see (Eq. (2))). In Figure 6b the very first doughnut-resized cell optimized for a typical area detector is shown: its cross section has been flattened starting from cell similar to the one in Figure 6a. To date doughnut and C-shaped cells up to 24 cm in diameter have been constructed. This size is currently limited by the volume of glass that can be maintained at the appropriate temperatures for forming it with a large propane/oxygen burner. We believe even larger cells can be produced by switching to a Hydrogen/oxygen burner that can produce higher temperatures.

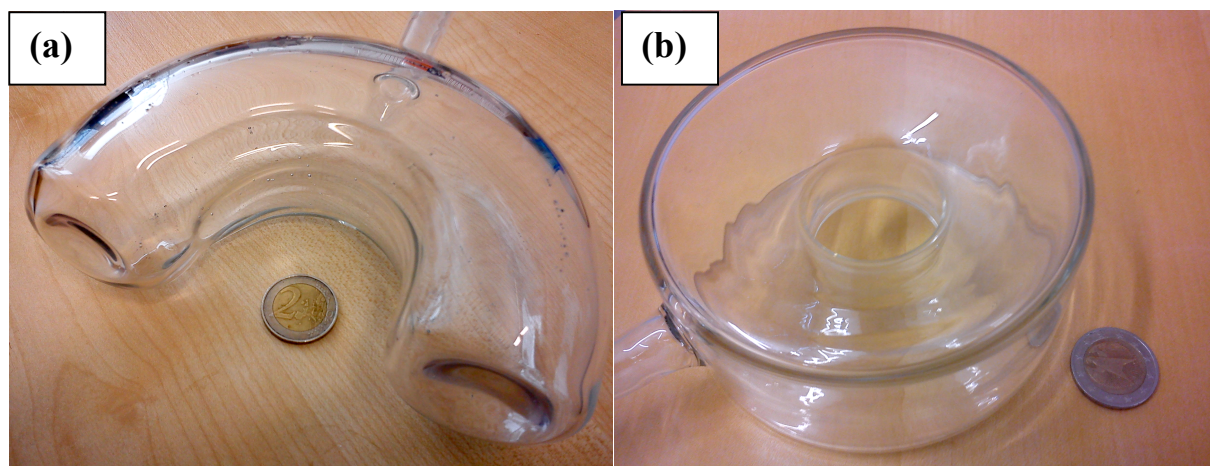


**Figure 5.** (a) A first C-shaped cell blank with a 6 cm diameter cross-section and 16.5 cm O.D. and (b) a doughnut cell blank of 12 cm O.D. and 6 cm high with more idealized trapezoidal cross-section geometry for the scattered beam.

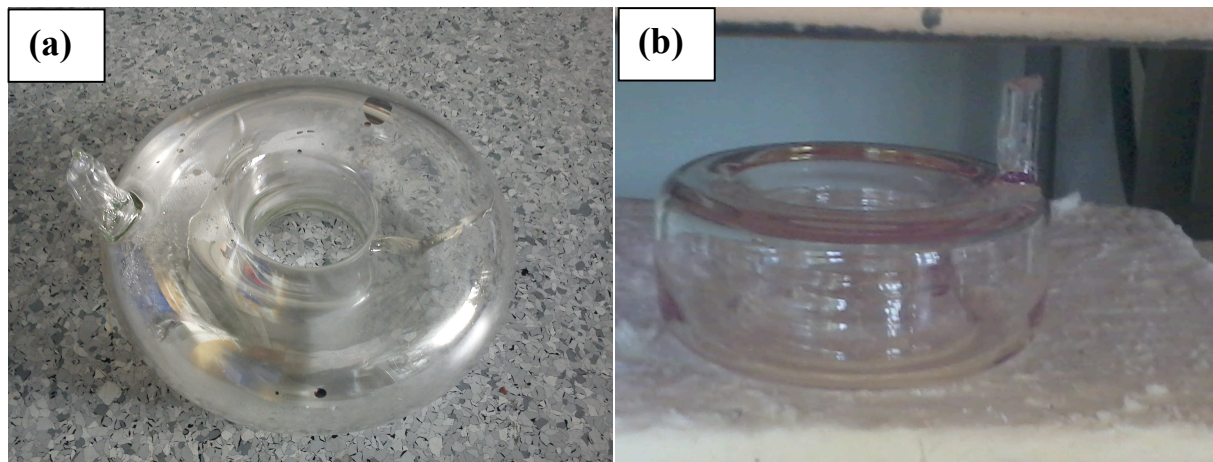


**Figure 6.** (a) The first filled doughnut shaped cell called Homer, 22 cm O.D. and 8 cm high with a circular or slightly D-shaped cross section for testing the Magic-PASTIS setup [20]. (b) A very large 22cm O.D. by 9 cm high doughnut cell and 9 cm I.D. inner hole with a trapezoidal cross section for the scattered neutron beam.

## 6. Conclusions.

The apparatus built to clean and fill SEOP cells operates routinely and we have produced several cells with lifetimes in the excess of several hundreds of hours. This now includes larger diameter cells, up to 12 cm I.D. that can be filled up to the gas pressure of 3.7 bar by submerging them into liquid N<sub>2</sub> while sealing them off. For some cells the obtained lifetime is about 800 hour per inverse bar, which means that we have approached the fundamental limit imposed by the dipole-dipole interaction of <sup>3</sup>He atoms. Currently all cells we fill use a K/Rb alkali-metal mixture allowing for higher optical pumping rates and is absolutely necessary to efficiently achieve high <sup>3</sup>He polarization in large cells.

## 7. Acknowledgments.

The authors would like to thank G. D’Orsaneo and A. Schwaitzer (Forschungszentrum Jülich glass workshop) and J. Anderson and A. Kirchoff (NIST glass workshop) for their help and advice and brainstorming concerning cell fabrication. We are also grateful to T. R. Gentile (NIST Physics Lab), W.C. Chen (NCNR), for their help and useful discussions.

The authors acknowledge funding by BMBF through the collaborative project 05E10CJ1. This research project has been also supported by the European Commission under the 7<sup>th</sup> Framework Programme thorough the ‘Research Infrastructures’ action of the ‘capacities’ Programme NMI3-II Grant number 283883.

## References

- [1] T. Walker and W. Happer, Spin-exchange optical pumping of noble-gas nuclei. *Rev Mod Phys*, vol. 69, no. 2, pp. 629–42, 1997.
- [2] F. D. Colegrove, L. D. Scheerer, and G. K. Walters, “Polarisation of helium-3 gas by optical pumping,” *Physical Review*, vol. 132, pp. 2561–2572, 1963.
- [3] J. Brossel, “Optical pumping in weak discharges.” *Fundamental Appl LASER Phys*, pp. 769–90, 1971.
- [4] W. Happer, E. Miron, D. Schreiber, and W. A. van Wijngaarden X. Zeng, “Polarization of the nuclear spins of noble-gas atoms by spin exchange with optically pumped alkali-metal atoms,” *Physical Review A*, vol. 29, no. 5, pp. 3092–3110, 1984
- [5] E. Babcock, S. Mattauch, A. Ioffe; High level of <sup>3</sup>He polarization maintained in an on-beam <sup>3</sup>He spin filter using SEOP, Original Research Article: *Nuclear Instruments and Methods in Physics Research*

Section A: Volume 625, Issue 1, 1 January 2011, Pages 43-46

- [6] S.R. Parnell, E.Babcock, K.Nunighoff, M.W.A.Skoda, S.Boag , S.Masalovich, W.C.Chen, R.Georgii, J.M.Wild, C.D.Frost; Study of spin-exchange optically pumped  $^3\text{He}$  cells with high polarisation and long lifetimes: Nuclear Instruments and Methods in Physics Research A 598 (2009) 774–778
- [7] M. Batz, S. Baeßler, W. Heil, E.W. Otten, D. Rudersdorf, J.Schmiedeskamp, Y. Sobolev, and M. Wolf:  $^3\text{He}$  Spin Filter for Neutrons; Journal of Research of the National Institute of Standards and echnology J. Res. Natl. Inst. Stand. Technol. 110, 293-298 (2005)
- [8] E. Babcock, B. Chann, T. G. Walker, W. C. Chen, and T. R. Gentile; Limits to the Polarization for Spin-Exchange Optical Pumping of  $\text{He}_3$ , Phys. Rev. Lett. 96, 083003 – Published 3 March 2006
- [9] N. R. Newbury, A. S. Barton, G. D. Cates, W. Happer, and H. Middleton. Gaseous  $^3\text{He}$ - $^3\text{He}$  magnetic dipolar spin relaxation. Phys. Rev. A, 48(6), 1993. doi:10.1103
- [10] G. D. Cates, S. R. Schaefer, and W. Happer. Relaxation of spins due to field inhomogeneities in gaseous samples at low magnetic fields and low pressure. Phys. Rev. A, 37, 1988.
- [11] G. D. Cates, D. J. White, T. Chien, S. R. Schaefer, and W. Happer. Spin relaxation due to inhomogeneous static and oscillating magnetic fields. Phys. Rev. A, 38, 1988.
- [12] R. Jacob, J. Teter, B. Saam, W. Chen, and T. Gentile, “Low-field orientation dependence of  $^3\text{He}$  relaxation in spin-exchange cells,” Physical Review A, vol. 69, pp. 021401–1–4, 2004.
- [13] J. Schmiedeskamp, W. Heil, E.W. Otten, R.K. Kremer, A. Simon, J. Zimmer, “Paramagnetic relaxation of spin polarized  $\text{He-3}$  at bare glass surfaces Part I,” European Physical Journal D, vol. 38, pp. 427-38, 2006.
- [14] R. E. Jacob, S. Morgan, B. Saam, and J. C. Leawoods, “Wall relaxation of  $^3\text{He}$  in spin-exchange cells,” Physical Review Letters, vol. 87, p. 143004, October 2001.
- [15] W. Heil, H. Humblot, E. Otten, M. Schafer, R. Sarkau, and M. Leduc, “Very long nuclear relaxation times of spin polarized helium-3 in metal coated cells,” Physics Letters A, vol. 201, pp. 337–343, 1995.
- [16] W. A. Fitzsimmons, L.L. Tankerslez, and G.K. Walters, “Nature of surface-induced nuclear spi-relaxation of gaseous  $^3\text{He}$ ,” Physical Review, vol. 179, pp. 156-65, 1969
- [17] A. Deninger, W. Heil, E.W. Otten, M. Wolf, R.K. Kremer, A. Simon, “Paramagnetic relaxation of spin polarized  $\text{He-3}$  at coated glass walls Part II,” European Physical Journal D, vol. 38, pp. 439-43, 2006
- [18] J. Schmiedeskamp, H.J. Elmers, W. Heil, E.W. Otten, Y. Sobolev, W. Kilian, H. Rinneberg, T. Sander-Thommes, F. Seifert, J. Zimmer, “Relaxation of spin polarized  $\text{He-3}$  by magnetized ferromagnetic contaminants Part III,” European Physical Journal D, vol. 38, pp. 445-54, 2006
- [19] W. C. Chen, T. R. Gentile, C. B. Fu, S. Watson, G. L. Jones, J. W. McIver and D. R. Rich, Polarized  $^3\text{He}$  cell development and application at NIST Journal of Physics: Conference Series 294 (2011) 12003
- [20] Stephen Boag: Spin Exchange Optical Pumping of  $^3\text{He}$  for Neutron Spin Filters, PhD Thesis, University of Nottingham (2008)
- [21] Strem chemical- <http://www.strem.com/>
- [22] KNF Neuberger- <http://www.knf.de/>
- [23] Z. Salhi, T. Großmann, M. Gueldner, W. Heil, S. Karpuk, E. W. Otten, D. Rudersdorf, R. Surkau, U. Wolf, Recycling of  $^3\text{He}$  from lung magnetic resonance imaging. Magnetic Resonance in Medicine Volume 67, Issue 6, pages 1758–1763, June 2012
- [24] A. Abragam, Principles of Nuclear Magnetism. London: Oxford University Press, 1966.
- [25] T. E. Chupp, J. D. Bowman, W. Chen, K. P. Coulter, M. Dabaghyan, T. Gentile, R. C. Gillis, G. L. Jones, M. Kandes, B. Lauss, S. I. Penttila, D. Rich, M. Sharma, T. B. Smith, A large area polarized  $^3\text{He}$  neutron spin filter, Nucl. Instr. Meth. A 574-500 (2007).
- [26] Yu. N. Pokotilovski, “Limits on short-range spin-dependent forces from spin relaxation,” Vol. 686, pp 114-7, 2010.
- [27] A.K. Petukhov, G. Pignol, and R. Golub, “Comments on ‘Limits on possible new nucleon monopole-dipole interactions from the spin relaxation of  $^3\text{He}$  gas,’” Physical Review D, vol. 84, p 058501, 2011.
- [28] Beecham, C. J.; Boag, S.; Frost, C. D.; et al.  $\text{He-3}$  polarization for ISIS TS2 phase I instruments PHYSICA B- Volume: 406 Issue: 12 Pages: 2429-2432 2011
- [29] Q. Ye, T.R. Gentile, J. Anderson, C. Broholm, W.C. Chen, Z. DeLand, R.W. Erwin, C.B. Fu, J. Fuller, A. Kirchhoff, J.A. Rodriguez-Rivera, V. Thampy, T.G. Walker, S. Watson, Wide Angle Polarization Analysis with Neutron Spin Filters, Physics Procedia, Volume 42, 2013, Pages 206-212, ISSN 1875-

- [30] A.K. Petoukhov, K.H. Andersen, D. Jullien, E. Babcock, J. Chastagnier, R. Chung, H. Humblot, E. Lelievre-Berna, F. Tasset, F. Radu, M. Wolff, H. Zabel, Recent advances in polarised  $^3\text{He}$  spin filters at the ILL, *Physica B* 385–386 (2006) 1146–1148
- [31] Z. Salhi, E. Babcock, A. Ioffe: ArXiv (2012) aeXiv:1201.5208